The black hole as a gravitational ‘‘lens’’

Hans C. Ohanian

Citation: American Journal of Physics **55**, 428 (1987); doi: 10.1119/1.15126
View online: https://doi.org/10.1119/1.15126
View Table of Contents: https://aapt.scitation.org/toc/ajp/55/5
Published by the American Association of Physics Teachers

Inserting this in (A6) yields the maximum cutoff frequency

$$\nu_{\max} = \frac{(1+\sqrt{\delta}\,)(1+\sqrt{\rho}\,)}{(1+\sqrt{\delta\rho}\,)}. \qquad \text{(A8)}$$

For $\delta = 1$, one finds $\nu_{\max} = 2$.

[a] Permanent address: Institute for Theoretical Physics, University of Düsseldorf, Düsseldorf, West Germany.

[1] F. L. Curzon and B. Ahlborn, Am. J. Phys. **43**, 22 (1975).
[2] M. H. Rubin, Phys. Rev. A **19**, 1272 (1979).
[3] R. D. Spence and M. J. Harrison, Am. J. Phys. **53**, 890 (1985).

The black hole as a gravitational "lens"

Hans C. Ohanian[a]
Istituto di Fisica "G. Marconi," Università di Roma, Italia and Specola Vaticana, Castel Gandolfo, Città del Vaticano, Italy

(Received 5 March 1986; accepted for publication 17 June 1986)

We discuss the "images" formed when the light from a distant source suffers a large deflection in the intense gravitational field in the immediate vicinity of a Schwarzschild black hole. The light can circle around the black hole one or several times, and therefore give rise to a sequence of images. We show that the deflection angles and the intensities of the images can be expressed in terms of elliptic integrals, leading to simple approximations in the limiting case of very large deflection angles.

I. INTRODUCTION

Most discussions of the gravitational "lens" effect[1] rely on the assumption that the gravitational field is weak and that the deflection angles of light rays are small. This approximation is adequate for the deflection produced by a star or by a galaxy, but not for that produced by a black hole. A light ray that enters the strong gravitational field near a black hole can be deflected through an arbitrarily large angle—in extreme cases, the light ray can circle around the black hole several times before proceeding outward. Thus, in contrast to the gravitational lens effect of stars or galaxies, the gravitational lens effect of a black hole does not require good alignment of light source, lens, and observer. Regardless of the position of the source, there are always some light rays that reach the observer after being deflected in the vicinity of the black hole, and the observer always sees multiple images when he looks toward the black hole—he sees an infinite sequence of images on each side of the black hole.

Detailed calculations of the lens effect produced by large deflections in the gravitational field of a maximally rotating black hole have been carried out by Cunningham and Bardeen,[2] who applied their results to the hypothetical case of a very massive black hole with a nearby orbiting star as light source. Although they were able to obtain a complete solution for the trajectories of light rays by means of first integrals of the equations of motion, their formulas are rather complicated because, in general, the trajectory does not remain in a plane. Here we will deal with the much simpler case of a black hole without rotation, i.e., a Schwarzschild black hole, for which the trajectory is planar.

Section II presents a calculation of the deflection of light rays and of the positions of the images seen by a distant observer. As shown by Darwin,[3] the deflection produced by a Schwarzschild black hole can be expressed in terms of an elliptic integral, i.e., it can be expressed in terms of a known, tabulated function. For the sake of simplicity, the distances from the black hole to the light source and to the observer will be taken as very large compared to the Schwarzschild radius; but this assumption is not essential.

Section III presents a calculation of the intensities of the images, compared to the intensity of the undisturbed light source. The images are always substantially fainter than the undisturbed light source, and their intensity decreases sharply with increasing deflection angle.[4] Section III takes advantage of an asymptotic approximation formula for the elliptic integral to establish that the intensity decreases exponentially with the deflection angle, if this angle is large.

In spite of the low intensity, the imaging of a light source by a large deflection in the gravitational field of a black hole may be indirectly observable. One promising candidate for such observations is the system SS 433. According to one model proposed for this system, the light comes from two small sources on a spinning disk near a black hole. Fang, Ruffini, and Stella[5] have remarked that light rays from each source could then reach an observer on the Earth either directly or after a large deflection around the black hole. Although the two images associated with these two light paths cannot be resolved, because their angular separation in the sky is too small, the second image can, in principle, be detected because its Doppler and redshift differs from that of the first image.

II. DEFLECTION OF LIGHT RAYS BY A BLACK HOLE

The first-order differential equation describing the trajectory of a light ray in the equatorial plane of a Schwarzs-

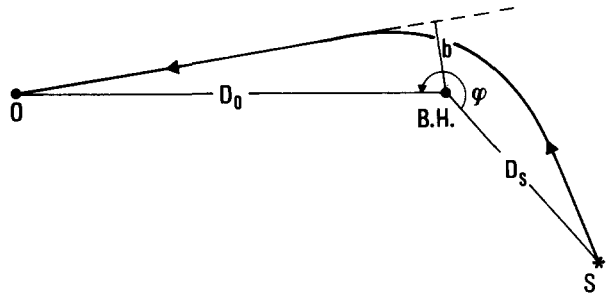

Fig. 1. Positions of source (S), black hole (B.H.), and observer (O). The angle ϕ shown here is the difference of azimuth between S and O.

child black hole is[6]

$$\frac{1}{b^2}-\left(\frac{du}{d\phi}\right)^2-u^2\left(1-\frac{2GMu}{c^2}\right)=0, \tag{1}$$

where ϕ is the azimuth angle and $u=1/r$. It is convenient to express all lengths in multiples of GM/c^2. With this choice of units,

$$\frac{1}{b^2}-\left(\frac{du}{d\phi}\right)^2-u^2(1-2u)=0. \tag{2}$$

Note that the spherical symmetry of the Schwarzschild solution entitles us to assume that the equatorial plane coincides with the plane determined by the positions of the light source, the center of the black hole, and the observer.

The constant b in Eq. (2) can be identified as the impact parameter; this becomes obvious in the limit $u\to 0$ (or $r\to\infty$), where Eq. (2) reduces to $1/b^2-(du/d\phi)^2=0$, which implies $u=\phi/b+\text{const.}$, as expected for a distant ($u\ll 1/b$) straight line of impact parameter b.

At the point of closest approach, $du/d\phi=0$. Designating this point by $u=\beta_2$, we see from Eq. (2) that

$$b=1/\sqrt{\beta_2^2(1-2\beta_2)}. \tag{3}$$

Equation (2) can be integrated directly to find the total change of azimuth angle (see Fig. 1) for a ray that arrives from $r=D_S$, bends around the black hole, and proceeds toward $r=D_O$. If D_S and D_O are much larger than b, the limits of integration can be extended to ∞ without significant loss of accuracy:

$$\phi=2\int_0^{\beta_2}\frac{du}{[1/b^2-u^2(1-2u)]^{1/2}}, \tag{4}$$

$$=2\int_0^{\beta_2}\frac{du}{[\beta_2^2(1-2\beta_2)-u^2(1-2u)]^{1/2}}. \tag{5}$$

Obviously, β_2 is one of the roots of the cubic polynomial $\beta_2^2(1-2\beta_2)-u^2(1-2u)$. If we designate the other roots by β_1 and β_3, we can write Eq. (5) as

$$\phi=\sqrt{2}\int_0^{\beta_2}\frac{du}{[(u-\beta_1)(u-\beta_2)(u-\beta_3)]^{1/2}}. \tag{6}$$

By comparing the cubic polynomials in Eqs. (5) and (6), we find that the roots β_1 and β_3 can be conveniently expressed in terms of β_2:

$$\beta_1=\tfrac{1}{2}\left[\tfrac{1}{2}-\beta_2+\sqrt{(\tfrac{1}{2}-\beta_2)(\tfrac{1}{2}+3\beta_2)}\,\right], \tag{7}$$

$$\beta_3=\tfrac{1}{2}\left[\tfrac{1}{2}-\beta_2-\sqrt{(\tfrac{1}{2}-\beta_2)(\tfrac{1}{2}+3\beta_2)}\,\right]. \tag{8}$$

A standard formula[7] permits the reduction of the integral (6) to an elliptic integral of the first kind

$$\phi=\frac{\sqrt{2}}{\lambda}F(\theta\backslash\alpha), \tag{9}$$

where

$$\lambda=\tfrac{1}{2}[(\tfrac{1}{2}-\beta_2)(\tfrac{1}{2}+3\beta_2)]^{1/4}, \tag{10}$$

$$\cos^2\theta=\frac{\frac{1}{2}-3\beta_2+4\lambda^2}{-\frac{1}{2}+3\beta_2+4\lambda^2}\,\frac{-\frac{1}{2}+\beta_2+4\lambda^2}{\frac{1}{2}-\beta_2+4\lambda^2}, \tag{11}$$

$$\cos^2\alpha=\frac{\frac{1}{2}-3\beta_2+4\lambda^2}{8\lambda^2}. \tag{12}$$

Equations (3) and (9) express b and ϕ in terms of the parameter β_2; these equations can be regarded as parametric equations determining ϕ as a function of b. With tabulated values of elliptic integrals, it is then straightforward to prepare a plot of ϕ vs b. In Fig. 2 we give a plot of $\phi-\pi$ vs b. The angle $\phi-\pi$ describes the misaligment of the source, the black hole, and the observer. We will call $\phi-\pi$ the *angular deviation*. It is approximately equal to the bending angle of the light ray if the distances D_S and D_O are large; more precisely

$$(\text{bending angle})=(\phi-\pi)+\frac{b}{D_S}+\frac{b}{D_O}. \tag{13}$$

The angular deviation approaches ∞ as b approaches $\sqrt{27}$, which corresponds to $\beta_2=1/3$ and to $\theta=\pi/2$, $\alpha=\pi/2$. A value of $r=1/u=3$ for the radius of closest approach corresponds to $r=3GM/c^2$ in conventional units. This is the radius of the photosphere, i.e., the radius at which a light ray follows a closed circular orbit around the black hole (this orbit is unstable).

For impact parameters near the critical value $b=\sqrt{27}$, interpolation on tables of elliptic integrals becomes unreliable, and it is convenient to use the following asymptotic approximation formula for the elliptic integral, valid for θ

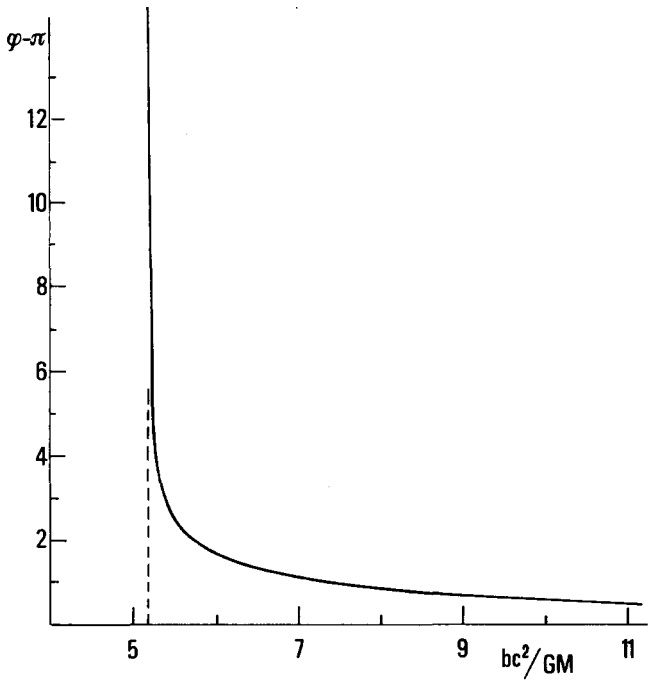

Fig. 2. Plot of the angular deviation $\phi-\pi$ vs impact parameter. For large values of the impact parameter, the angular deviation is approximately $4GM/bc^2$.

and α near $\pi/2$:

$$F(\theta\setminus\alpha)\cong[1+\tfrac{1}{4}(\pi/2-\alpha)^2]\times\ln\tan[\pi/2-\tfrac{1}{4}(\pi/2-\theta)\times\tfrac{1}{4}\sqrt{(\pi/2-\theta)^2+(\pi/2-\alpha)^2}]\,. \quad (14)$$

(This approximation can be obtained from the ascending Landen transformation,[7] retaining only one term.) For β_2 near 1/3, Eqs. (11) and (12) yield the approximations $(\pi/2-\theta)^2\cong 2(1/3-\beta_2)$ and $(\pi/2-\alpha)^2\cong 4(1/3-\beta_2)$, and therefore Eq. (14) leads to

$$\phi\cong 4\ln\tan[\pi/2-(\sqrt{2}/4)(1+\sqrt{3})\sqrt{1/3-\beta_2}]\,. \quad (15)$$

This formula will prove useful in the next section, for estimating the intensity of the faint images near the critical impact parameter.

If the light source, the black hole, and the observer are *not* aligned, then there is always a (almost straight) light ray that reaches the observer without passing near the black hole; we will ignore this ray. All the other rays that reach the observer must pass near the black hole, and they give rise to a sequence of images seen in the sky near the black hole. The observer sees the first such image at an angular position $b(\phi_1)/D$ to one side of the black hole, where $b(\phi_1)$ is the impact parameter corresponding to the azimuth angle ϕ_1, as shown in Fig. 1. He sees other images at $b(\phi_2)/D$, $b(\phi_3)/D$, $b(\phi_4)/D$, etc., where $\phi_n=\phi_1+2\pi(n-1)$. Besides this sequence of images, all of which are produced by light rays circling around the black hole in the same direction (counterclockwise in Fig. 1), there is a second sequence of images on the other side of the black hole, produced by light rays circling the black hole in the opposite direction (clockwise in Fig. 1). The angular positions of these images are $b(\phi_1')/D$, $b(\phi_2')/D$, etc., with $\phi_n'=2\pi(n'+1)-\phi_1$. Obviously, the deflection angles ϕ_1 and ϕ_1' are the smallest, and, as will be shown in Sec. III the intensities of these two images are the largest.

Figure 3 displays the positions of the sequences of images, for the special case $\pi-\phi=45°=\pi/4$. The circle is the photosphere, of angular radius $\sqrt{27}\,GM/D_Oc^2=(5.196...)GM/D_Oc^2$. The numbers next to the images give angular positions relative to the center of the black hole, in units of GM/D_Oc^2. The positions of the images with $n>3$ and with $n'>2$ are very near the circle of angular radius $\sqrt{27}GM/D_Oc^2$; these higher-order images have not been included in the diagram.

Incidentally, the "images" of a gravitational "lens" merely correspond to directions of incidence of rays on the observer. The "images" are *not* points from which a bundle of (extrapolated) rays appears to diverge. This can be recognized by noting that in a small bundle of rays arriving from the source, the backward extrapolation of a pair of rays diverging perpendicularly out of the equatorial plane shown in Fig. 1 yields a point of intersection lying ahead of the black hole, on the extended line from the source to the black hole, whereas the backward extrapolation of a pair of rays diverging within the equatorial plane of Fig. 1 yields a point of intersection beyond the black hole. Thus different rays in the bundle appear to come from different points, and the gravitational "lens" forms no true image (stated in another way: the image has no well-defined parallax). The only true image formed in the gravitational "lens" effect is the image formed in the eye of the observer or on his photographic film. Since astronomical distances are extremely large, such an image corresponds to a given direction of incidence of light from the sky.

III. INTENSITY OF IMAGES

The intensity of the image is conveniently described by the gain factor, i.e., the factor by which the observed intensity of the image produced by the gravitational lens is larger than that of the source when by itself (in our case, the gain factor is usually less than one). We will assume that the source is a small sphere of angular diameter ω when by itself, and that it radiates isotropically, with uniform surface brightness. (Alternatively, we could assume that the source is a small disk, but then we would have to make an allowance for the change of angle of view produced by the deflection of the light rays.) When the rays from the source are undisturbed, the observer sees a small bright disk of angular diameter ω in the sky; when the rays from the source are deflected by the black hole, the observer sees an image in the form of a small ellipse. It follows from the Liouville theorem that the surface brightnesses of the source and of the image are the same[8]; hence the gain factor is simply equal to the ratio of the solid angle subtended by the image to the solid angle subtended by the source. Figure 4 shows the source and the black hole, and two rays from opposite edges of the source to the observer. The linear size of the source is $D_{OS}\omega$ where D_{OS} is the distance from the source to the observer. Hence the angular width

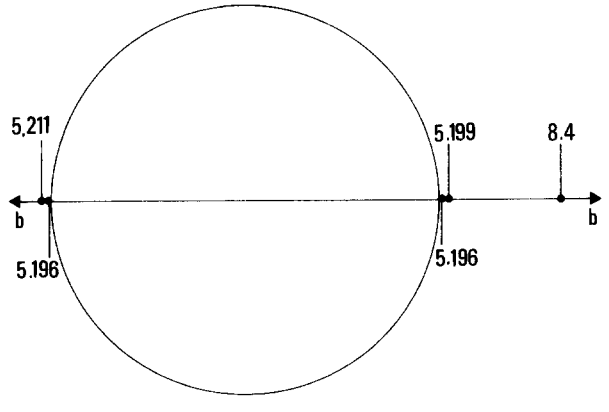

Fig. 3. Positions of the images seen in the sky near the black hole. Distances in this diagram are proportional to angular distances seen in the sky. The circle represents the photosphere, with a radius $\sqrt{27}=5.196...$.

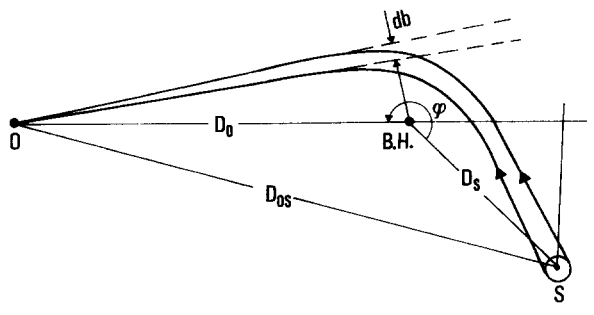

Fig. 4. Two light rays from opposite edges of the source toward the observer. The difference between the impact parameters of the light rays is *db*.

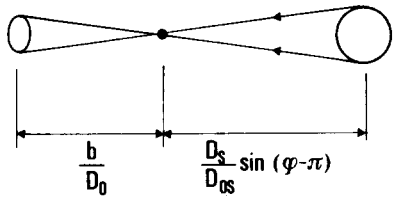

Fig. 5. Source, black hole, and image as seen in the sky. The image is (approximately) a small ellipse. The distances marked in this diagram are angular distances, as seen by the observer.

seen from the black hole is

$$d\phi = \frac{D_{OS}}{D_S}\omega.$$

The angular width of the image seen by the observer is $-db/D_O$, or $|db|/D_O$ (as shown in Fig. 4, db is negative when $d\phi$ is positive). Thus the gain factor for the angular size in the equatorial plane is

$$\frac{|db|/D_O}{\omega} = \frac{|db|/D_O}{(D_S/D_{OS})d\phi} = \frac{1}{D}\frac{1}{|d\phi/db|}, \tag{16}$$

where $D = D_O D_S/D_{OS}$. Next, we must consider the gain factor for the angular size perpendicular to the equatorial plane. Figure 5 shows the source, the black hole, and the image as seen from the position of the observer. From this figure we recognize that the gain factor for the perpendicular angular size is

$$\frac{b/D_O}{(D_S/D_{OS})|\sin(\phi-\pi)|} = \frac{b}{D|\sin(\phi-\pi)|}. \tag{17}$$

The gain factor for the solid angle, and therefore the gain factor for the intensity, is the product of (16) and (17):

$$(\text{gain}) = \frac{1}{D^2}\frac{b}{|\sin(\phi-\pi)d\phi/db|}. \tag{18}$$

In conventional units this is best written as the product of two dimensionless factors:

$$(\text{gain}) = \frac{(GM/c^2)^2}{D^2}\frac{bc^2/GM}{|\sin(\phi-\pi)(GM/c^2)d\phi/db|}. \tag{19}$$

Here the factor $(GM/c^2)^2/D^2$ is the same for all the images in the sequences of images shown in Fig. 3, whereas the remaining factor varies drastically from one image to the next.

For the calculation of the gain factor, we need to find the derivative $d\phi/db$, which involves derivatives of the elliptic integral $F(\theta\backslash\alpha)$ with respect to θ and to α. The latter derivative can be expressed in terms of an elliptic integral of the second kind, $E(\theta\backslash\alpha)$. The result is

$$\frac{d\phi}{db} = -\frac{\sqrt{2}}{\lambda^2}F\frac{d\lambda}{db} + \frac{\sqrt{2}}{\lambda}\frac{1}{(1-\sin^2\alpha\sin^2\theta)^{1/2}}\frac{d\theta}{db} + \frac{\sqrt{2}}{\lambda}\left(F + \frac{E-F}{\sin^2\alpha} - \frac{\sin\theta\cos\theta}{(1-\sin^2\alpha\sin^2\theta)^{1/2}}\right)\tan\alpha\frac{d\alpha}{db},$$

where the derivatives $d\lambda/db$, $d\theta/db$, and $d\alpha/db$ must be evaluated from Eqs. (10)–(12) (for the sake of brevity, we omit the expressions for these derivatives).

Figure 5 shows a plot of the gain factor as a function of the angular deviation. The sharp spikes at $\phi - \pi = 2\pi n$ correspond to alignment of the source, black hole, and observer; this places the observer on a caustic, where there is a strong concentration of rays, which the observer sees arriving from a bright annulus that appears to surround the black hole. The intensity on this caustic is large, but not infinite; the intensity attains a maximum value that depends on the size of the source, or, if the source is effectively pointlike, a maximum value that depends on diffraction effects.[9]

If the angle ϕ is large, we can obtain a simple approximation of $d\phi/db$ by differentiating Eq. (15), and then using Eq. (15) once more to eliminate $1/3 - \beta_2$:

$$\frac{d\phi}{db} = -\frac{1}{27\times 32}\frac{(1+\sqrt{3})^4}{(\sqrt{3})^3}e^{\phi}. \tag{20}$$

This leads to a gain factor

$$(\text{gain}) = \frac{32\times 9^3}{(1+\sqrt{3})^4}\frac{1}{D^2}\frac{e^{-\phi}}{|\sin(\phi-\pi)|}. \tag{21}$$

This is a good approximation (within a few percent) whenever the angle ϕ is in excess of 3π. According to Eq. (21), the intensities of successive images in the sequence shown in Fig. 3 decrease by factors of $e^{-2\pi}$. Thus, the sum of the

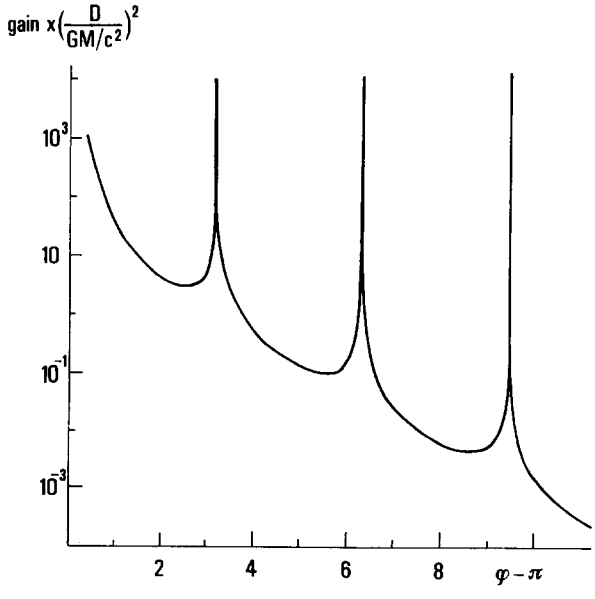

Fig. 6. Plot of the gain factor as a function of the angular deviation.

Table I. Gain factors.

n or n'	$\phi - \pi$	gain
1	$\pi/4$	2.9×10^{-2}
2	$9\pi/4$	8.8×10^{-6}
3	$17\pi/4$	1.6×10^{-8}
1′	$7\pi/4$	4.2×10^{-5}
2′	$15\pi/4$	7.8×10^{-8}

intensities of all the images starting with, say, the third image equals the intensity of the third image multiplied by a factor[10]

$$1 + e^{-2\pi} + e^{-4\pi} + \cdots = \frac{1}{1 - e^{-2\pi}}. \tag{22}$$

This shows that the sum of the intensities of the infinite sequence of images is not significantly different from the intensity of the first term in the sum, i.e., the images beyond the third contribute very little to the net intensity.

For a more or less realistic example of the intensities that can be attained by rays that have been subjected to large deflections, consider a source at a distance $D = 50GM/c^2$, as suggested in the disk model of Fang, Ruffini, and Stella for SS 433. If the source is displaced by an angle of 45° from alignment (i.e., $\phi - \pi = \pi/4$), then the gain factors for the first, second, and third images on one side of the black hole, and for the first and second images on the other side are as listed in Table I. The first of these images, with an intensity of about 2.9% of the undisturbed intensity, is possibly within the range of what is detectable; the other images are too faint.

ACKNOWLEDGMENTS

I am grateful to Dr. G. V. Coyne, S. J., and the staff of the Vatican Observatory for their kind hospitality at Castel Gandolfo.

[a] Present and permanent address: Rensselaer Polytechnic Institute, Troy, NY 12180.

[1] A. Einstein, Science **84**, 506 (1936); F. Zwicky, Phys. Rev. Lett. **51**, 290 (1937); S. Liebes, Phys. Rev. **133B**, 835 (1964); S. Refsdal, M. N. R. S. **128**, 290 (1964); see also R. R. Bourassa, R. Kantowski, and T. D. Norton, Ap. J. **185**, 747 (1973); and R. R. Bourassa and R. Kantowski, Ap. J. **195**, 13 (1975) and references cited therein. The paper by Bourassa and Kantkowski gives a complete treatment of the case of a spheroidal gravitational lens.

[2] C. T. Cunningham and J. M. Bardeen, Ap. J. **183**, 237 (1973).

[3] C. G. Darwin, Proc. R. Soc. A **249**, 180 (1959). A brief summary of Darwin's results is given in C. W. Misner, K. S. Thorne, and J. A. Wheeler, *Gravitation* (Freeman, San Francisco, 1973), Fig. 25.7. I thank the referee for bringing these references to my attention.

[4] The intensities for the first three images are stated in Misner, Thorne, and Wheeler, *Gravitation*, exercise 25.26.

[5] L. Z. Fang, R. Ruffini, and L. Stella, Vistas Astron. **25**, 185 (1981). See also R. Ruffini, D. J. Song, and L. Stella, Astron. Astrophys. **103**, L7 (1981).

[6] See, e.g., Misner, Thorne, and Wheeler, *Gravitation*, Eq. (25.57).

[7] M. Abramowitz and I. A. Steigman, *Handbook of Mathematical Functions* (National Bureau of Standards, Washington, DC, 1964), p. 597.

[8] See, e.g., E. Fermi, *Nuclear Physics* (University of Chicago Press, Chicago, 1950), pp. 232–233.

[9] For caustics and diffraction effects in gravitational lenses, see H. C. Ohanian, Ap. J. **271**, 551 (1983), and references cited therein.

[10] We assume that the coherence length of the light is small compared to GM/c^2, so that the intensities, rather than the amplitudes, of the images behave additively.

Approximations for the range of ballistic missiles

Ralph Snyder

Department of Physics, University of Connecticut, Storrs, Connecticut 06268

(Received 9 January 1986; accepted for publication 2 July 1986)

The actual range, flight time, and maximum height of an ICBM are compared to the predictions of five simple approximations that are more sophisticated than the standard flat-Earth-with-constant-gravity problem but more elementary than the full Keplerian solution. The simplest of these approximations is accessible to first-year students and gives results in closed form whose range predictions are in good agreement with the Keplerian ranges at typical ICBM speeds.

I. INTRODUCTION

If a projectile is launched from the surface of the Earth with an initial speed V at an angle α with the horizontal, how far will it travel before returning to Earth? And what optimum angle, α_0, will give the maximum range for a fixed V? Every course in elementary mechanics derives the answers to these questions under the assumptions of a flat Earth with constant gravity: $V^2 \sin 2\alpha/g$, and 45°. But at the high speeds characteristic of modern ballistic missiles, thousands of meters per second, the effect of the Earth's curvature and of the inverse-square law rapidly vitiate those elementary results: they are off by nearly a factor of 2 under typical ICBM conditions. The correct results are readily obtained of course; the trajectory is a segment of a Keplerian ellipse with the Earth's center at one focus. To derive the equation for the range (and height and flight time) is a straightforward exercise in intermediate mechanics.

This article discusses five exercises which enrich the standard projectile problem by loosening the flat-Earth-with-constant-gravity restriction, but without solving the complete Kepler problem. After background work in Sec. II, Sec. III presents a very short and direct derivation of an improved formula for the range, using, in addition to the standard flat-Earth derivation, only the freshman-level concept of centripetal acceleration. The results turn out to be surprisingly successful in reproducing the actual range of an ICBM trajectory and in fact predict the *exact* value of α_0. Next, Sec. IV reexamines the problem in more detail by considering the centrifugal and coriolis forces in a frame of reference that is rotating with the missile so that the initial velocity is purely vertical in that frame. The results of Sec. III are recovered when the coriolis force is omitted; including the coriolis force gives results which elucidate the cancellations which led to III's accurate results. Section V discusses a simple exercise which looks at the effects of the inverse-square law alone, separated from curvature effects.